UPPSALA
UNIVERSITET

UPTEC F 22043
Examensarbete 30 hp
Juni 2022

Genuine geometric quantum gates induced by non-cyclic geodesic evolution of computational basis

Nils Eivarsson

Civilingenjörsprogrammet i teknisk fysik

UPPSALA
UNIVERSITET

Genuine geometric quantum gates induced by non-cyclic geodesic evolution of computational basis

Nils Eivarsson

Abstract

To reach the error threshold required to successfully perform error correcting algorithms in quantum computers, geometric quantum gates have been considered because of their natural resilience against noise. Non-cyclic geometric gates have been proposed to reduce the run time of conventional geometric gates, to further guard against decoherence. However, while these proposed gates remove the dynamical phase from the computational basis, they do not in general remove it from the eigenstates of the time evolution operator. For a non-cyclic gate to genuinely be considered geometric the dynamical phase should be removed from both the computational basis and the eigenstates. Here, a scheme for finding genuine non-cyclic geometric gates is proposed. The gates are designed to evolve the computational basis along non-cyclic paths, consisting of two geodesic segments, chosen such that the dynamical phase is removed from the eigenstates. The gates found with this scheme did not have shorter run times than cyclic gates, but it was possible to implement any gate with this scheme. The findings are important for the understanding of how general quantum computations can be implemented with geometric gates.

Teknisk-naturvetenskapliga fakulteten

Uppsala universitet, Utgivningsort Uppsala

Handledare: Erik Sjöqvist Ämnesgranskare: Vahid Azimi Mousolou

Examinator: Tomas Nyberg

Populärvetenskaplig sammanfattning

En kvantdator är en beräkningsmaskin som är grundad i kvantmekanik för att utföra dess beräkningar. Tack vare att dessa enheter är kvantmekaniska, tillkommer egenskaper som superposition, att en partikel kan befinna sig i flera tillstånd samtidigt, och kvantsammanflätning, ett sätt på vilket partiklar kan sammanlänkas med varandra. Med hjälp av dessa egenskaper kan en kvantdator utföra algoritmer i vissa fall betydligt snabbare än motsvarande algoritmer på en vanlig dator. Därför önskar man att kunna utnyttja den enorma beräkningskraften som kvantdatorer skulle kunna ha. Det finns dock hinder som måste lösas innan dagens kvantdatorer skulle ge en beräkningsmässig vinst över klassiska datorer. Dels skulle de behöva ha fler kvantbitar, kvantdatorns motsvarighet till en bit i en klassisk dator, för att kunna göra beräkningar i större skala och de skulle behöva vara mer robusta mot fel. Kvanttillstånd är känsliga mot brus vilket sätter stora krav på att kvantdatorer ska vara tåliga mot bruset för att informationen i kvantbitarna inte ska gå förlorad.

En idé för att reducera bruset i en kvantdator är att använda sig av geometriska kvantgrindar. Kvantgrindar är enkla operationer som förändrar kvantbitens tillstånd, de är kvantdatorns motsvarighet till logiska grindar i en klassisk dator. En given kvantberäkning är ett specifikt nätverk av kvantgrindar. Geometriska grindar är en speciell typ av kvantgrindar som bygger på konceptet geometrisk fas. När en partikels tillstånd ändras cykliskt skiljer sig start- och sluttillståndet med en fas som kan delas upp i två delar: en dynamisk och en geometrisk fas. Den geometriska fasen beror enbart på vägen längs vilken partikelns tillstånd utvecklats, men inte på hur snabbt utvecklingen skedde. Genom design av tidsutveckling kan den dynamiska fasen elimineras och fasen som partikeln får efter utvecklingen är då rent geometrisk. Geometriska grindar är kvantgrindar som endast bygger på geometrisk fas och blir därigenom naturligt tåliga mot brus.

För varje tidsutveckling av en kvantbit kommer det finnas tillstånd som ändras cykliskt, alltså börjar och slutar i samma tillstånd, men med en fasskillnad. Dessa tillstånd definierar egentillstånden till tidsutvecklingen. För att en kvantgrind ska vara en geometrisk grind måste alltså den dynamiska fasen elimineras från egentillstånden. Även tillstånd andra än egentillstånden kommer att få en fas när de genomgår samma tidsutveckling trots att dessa inte kommer utvecklas cykliskt, utan kommer ändras till ett annat sluttillstånd än starttillståndet. Uppdelningen av geometrisk och dynamisk fas går även att göra för de icke-cykliska utvecklingarna.

För att tillverka grindar som opererar snabbare finns det än önskan att hitta geometriska grindar baserade på icke-cykliska banor. I tidigare studier har tidutvecklingar som eliminerar den dynamiska fasen från beräkningsbasen studerats. Beräkningsbasen är två valda ortogonala tillstånd hos en kvantbit som representerar en boolesk 1:a respektive 0:a. Trots att den dynamiska fasen har eliminerats för beräkningsbasen i dessa fall har egentillstånden till tidsutvecklingarna inte tagits i åtanke och genomgår generellt inte rent geometriska utvecklingar. Det är därför oklart om dessa tidigare studerade realiseringar verkligen kan kallas geometriska grindar.

I denna rapport undersöktes utvecklingar där beräkningsbasen rör sig i specifika icke-cykliska banor som garanteras vara fria från dynamiska faser. Genom att variera parametrar som specificerar dessa banor gick det att eliminera de dynamiska faserna även från egentillstånden. Med detta går det att visa att det är möjligt att konstruera genuint geometriska grindar som är icke-cykliska. Detta är viktigt för att förstå hur generella kvantdatorer kan implementeras med geometriska grindar, och därigenom ta steg närmre en fullt fungerande kvantdator.

1 Introduction

Quantum computation is a form of computation which uses properties of quantum mechanics, such as superposition and entanglement, to be able to perform calculations. By use of these properties, some quantum computational algorithms can outperform equivalent classical algorithms. A famous example of this is Shor's algorithm [1] for finding prime factors. This is an algorithm which can find prime numbers exponentially faster than any algorithm a classical computer can run. A quantum computer with sufficiently many qubits, the quantum computer's equivalent to bits, running this algorithm would be able to break common public-key cryptography schemes, such as RSA, which are deemed secure today [2]. This shows the incredible computational potential of these devices.

The quantum computers of today do not have the number of qubits required to break these cryptography schemes but every year a new record is set, moving us closer to the goal. It is not, however, enough to scale up quantum computers, they also need to be resilient to noise and decoherence. Quantum decoherence is when a quantum state is changed due to interactions with an external system, leading to the state losing its quantum mechanical properties. The computational state within a quantum computer cannot be completely isolated and decoherence is therefore inevitable. It is possible to overcome this issue according to the error threshold theorem [2]. It states that a quantum computer with an error rate below a threshold will be able to suppress the errors, induced by noise and decoherence, with quantum error correction algorithms.

One approach to reach this error rate threshold is to use geometric quantum logic gates [3]. They are based on the concept of geometric phases of quantum systems [4]. When a quantum state undergoes a cyclic evolution it can gain a phase factor. This phase factor can be split into a dynamical part and a geometric part, where the geometric part is only dependent on the path a quantum state takes through its state space. By choosing an evolution where the dynamical phases are trivial this can be used to implement quantum logic gates which are purely dependent on the geometry of the path. This dependency on only geometry can be shown to be naturally resilient against certain types of noise. [5]

While geometric quantum gates show promise in the implementation of robust quantum computers there are still improvement to be made before they are fully operational. One possible improvement is to reduce the run time of the gates, as faster operation time would reduce the qubits' exposure to the environment, and thereby reduce the decoherence. To reduce the run time, some ideas to use non-cyclic evolution in the implementation of geometric quantum gates have been proposed [6–8]. These gate are based on qubits evolving along open paths while still only acquiring a geometric phase. However, in cyclic evolution of the computational states the geometric phases are the eigenvalues of the time evolution operator but this is in general not the case for the non-cyclic case. This makes the geometric meaning of these non-cyclic gates ambiguous. In this report, we propose an approach of realizing time efficient geometric gates by finding gates where the dynamical phase is removed for the eigenstates of the time evolution operator while the computational states undergo geometric non-cyclic evolution.

1.1 Objective

This project will examine single qubit gates where the computational basis evolves along non-cyclic paths constructed with geodesic segments. The gates will be examined to find for which paths the evolution of the eigenvectors of the time evolution operator becomes geometric. This is done by calculating the eigenvalues and eigenstates of a general gate and then searching for which set of parameters the dynamical phase of the evolution becomes trivial.

The project is limited to only studying gates using two pulses to drive the qubit, since two pulses is the minimum required to make any meaningful geometric gates. Each pulse needs to be fine-tuned to avoid noise, making a gate with more pulses harder to implement noiselessly. More pulses also increase the degrees of freedom for what paths are possible, giving more freedom in choosing the evolution but making it harder to study the gates systematically due to the increasing number of pulse parameters.

2 Quantum Computation

2.1 Qubit

The basis of quantum computation is the qubit [2]. The qubit is a two-state quantum mechanical system where one state represents a boolean 0 and the other a 1. These are two orthogonal quantum states and are usually expressed in the Dirac notation as: $|0\rangle$, $|1\rangle$. The $|\rangle$-bracket, called a ket, signifies that these are complex vectors. There is also the $\langle|$-bracket, called a bra, which is the transposed complex conjugate of the ket. The set of $\{|0\rangle, |1\rangle\}$ is called the computational basis and span the vector space of the qubit. Since the qubit is quantum mechanical it can be in a superposition of the two states. A general qubit state is therefore of the form

$$|\psi\rangle = \alpha\,|0\rangle + \beta\,|1\rangle\,, \tag{1}$$

where α and β are two complex numbers with $|\alpha|^2$ and $|\beta|^2$ describing the probability of measuring respective state. Therefore, α and β have the restriction $|\alpha|^2 + |\beta|^2 = 1$.

An intuitive way of visualising a qubit is the Bloch sphere, where each state is represented by a point on a unit sphere, as shown in Fig. 1. The qubit is projected on the Bloch sphere by

$$\begin{aligned} \alpha &= e^{i\gamma}\cos\left(\frac{\theta}{2}\right), \\ \beta &= e^{i\gamma+\varphi}\sin\left(\frac{\theta}{2}\right). \end{aligned} \tag{2}$$

Here, θ is the angle from the north pole, meaning the north pole is the $|0\rangle$ state and the south pole is the $|1\rangle$ state. γ is a global phase and φ is the relative phase of the two basis states. The global phase factor has no observable effect in a quantum system and can therefore be ignored. Experimentally, qubits can be implemented in a variety of ways, such as trapped ions [9], nitrogen vacancies in diamonds [10], or superconducting circuits [11].

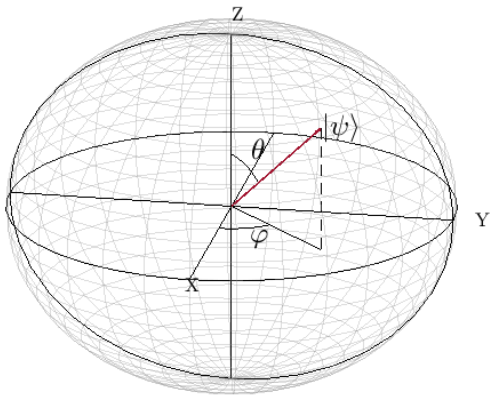

Figure 1: A state $|\psi\rangle$ on the Bloch sphere

2.2 Quantum logic gates

Quantum computation is performed by letting quantum logic gates transform the qubits, similarly to logic gates in a classical computer. They transform qubits from one state to another in the form of unitary operators. They can be represented by a matrix relative some basis, usually the computational basis.

One of the most important quantum gates is the Hadamard gate (H) which preforms the mapping $|0\rangle \to \frac{|0\rangle+|1\rangle}{\sqrt{2}}$ and $|1\rangle \to \frac{|0\rangle-|1\rangle}{\sqrt{2}}$ and thereby transforming the two basis states of the computational basis into a equally probable superposition of the two states. One way of implementing this gate is a π-rotation around the axis $\frac{\vec{x}+\vec{z}}{\sqrt{2}}$ on the Bloch sphere. In the computational basis it is represented by the Hadamard matrix.

$$\mathrm{H} = \frac{1}{\sqrt{2}}\begin{pmatrix} 1 & 1 \\ 1 & -1 \end{pmatrix}. \tag{3}$$

Other important quantum gates are the Pauli gates also called the X-, Y-, and Z-gates. These are gates based on the Pauli matrices, three 2×2 linearly independent and traceless matrices important for quantum mechanics. They where originally introduced in the mathematical treatment of spin precession but has subsequently become extremely useful in quantum computing. These matrices are

$$\sigma_x = \mathrm{X} = \begin{pmatrix} 0 & 1 \\ 1 & 0 \end{pmatrix}, \quad \sigma_y = \mathrm{Y} = \begin{pmatrix} 0 & -i \\ i & 0 \end{pmatrix}, \quad \sigma_z = \mathrm{Z} = \begin{pmatrix} 1 & 0 \\ 0 & -1 \end{pmatrix}. \tag{4}$$

They are equivalent to rotations around the x-, y-, and z-axis on the Bloch sphere by π radians. The X-gate is also referred to as the NOT-gate since it maps to $|0\rangle \to |1\rangle$ and $|1\rangle \to |0\rangle$, similarly to the classical NOT-gate.

One last important single qubit quantum gate is the T-gate, also called the $\pi/8$-gate. This gate shifts the phase φ of the qubit with $\pi/4$ radians. The matrix representation of

this gate is

$$\mathrm{T} = \begin{pmatrix} 1 & 0 \\ 0 & e^{i\pi/4} \end{pmatrix} = e^{i\pi/8} \begin{pmatrix} e^{-i\pi/8} & 0 \\ 0 & e^{i\pi/8} \end{pmatrix}. \tag{5}$$

The operation is a $\pi/4$-rotation around the z-axis. The $\pi/8$ name comes from the second definition of the the T-gate seen in Eq. (5) but since global phase has no measurable significance the two operations are equivalent.

For quantum computation it is also necessary for the qubits to interact with each other with controlled operations. The most common controlled operation is the controlled NOT gate (CNOT). The CNOT is a two-qubit gate that performs the NOT operation on a target qubit when a control qubit is in the $|1\rangle$-state, while it leaves the target unaffected if the control qubit is in the $|0\rangle$-state. In the computational basis of $\{|00\rangle, |01\rangle, |10\rangle, |11\rangle\}$, where the first number is the control qubit and the second is the target qubit, the CNOT-gate takes the form

$$\mathrm{CNOT} = \begin{pmatrix} 1 & 0 & 0 & 0 \\ 0 & 1 & 0 & 0 \\ 0 & 0 & 0 & 1 \\ 0 & 0 & 1 & 0 \end{pmatrix}. \tag{6}$$

These interactions allow the qubits to become entangled, which is a crucial feature of quantum computation.

The experimental implementation of quantum gates depends on what qubit setup is used. For example, in trapped ions short laser pulses are used [9], while for superconducting qubits it is common to use microwave pulses [11].

2.3 Universal quantum gates

To make quantum computing practically implementable, it is desired to find sets of gates which can be combined to replicate any gate. In classical computing there are gates such as the NAND and NOR gates which alone fulfill this desire, meaning all boolean functions can be implemented using only one of these. In quantum computing there is no single gate which fulfill this but there are sets of gates which do, one such set is the set {H, T, CNOT}. A set of quantum gates, such as this, is called a set of universal quantum gates meaning that all other gates can be simulated with a combination of gates from this set to an arbitrary accuracy. This condition of arbitrary accuracy is added because, unlike a classical computer, a quantum computer is not discrete and with this an uncountable number of gates are possible. Therefore, an uncountable set of gates would be required to simulate a quantum computation exactly but a finite set of gates picked from a universal set can simulate a quantum computation to a chosen degree of accuracy.

3 Geometric phase gates

To understand geometric quantum gates some insight into quantum evolution is first required.

3.1 Quantum evolution

The evolution of a quantum system in time is governed by the unitary time evolution operator $\mathcal{U}(t, t_0)$ [12] as

$$|\psi(t_0 : t)\rangle = \mathcal{U}(t, t_0)\,|\psi(t_0)\rangle\,. \tag{7}$$

It describes how the state evolves from a time t_0 to a time t. The operator $\mathcal{U}$ is a solution of the Schrödinger equation

$$i\hbar\frac{\partial}{\partial t}\mathcal{U}(t, t_0) = \mathcal{H}(t)\,\mathcal{U}(t, t_0), \tag{8}$$

where $\mathcal{H}(t)$ is the Hamiltonian of the system. For a piecewise time-independent Hamiltonian the solution takes the form

$$\mathcal{U}(\tau, 0) = \mathcal{U}_n(\tau, t_{n-1})\,\mathcal{U}_{n-1}(t_{n-1}, t_{n-2})\cdots\mathcal{U}_2(t_2, t_1)\,\mathcal{U}_1(t_1, 0), \tag{9}$$

and each $\mathcal{U}_m$ is

$$\mathcal{U}_m(t_m, t_{m-1}) = \exp\left[\frac{-i\mathcal{H}_m(t_m - t_{m-1})}{\hbar}\right], \tag{10}$$

with $\mathcal{H}_m$ being a time-independent Hamiltonian, and $t_n \equiv \tau$. This operator can be written into diagonal form by using the relation

$$\mathcal{U}(t_m, t_{m-1}) = \sum_k |\psi_k\rangle \exp\left[\frac{-iE_k(t_m - t_{m-1})}{\hbar}\right]\langle\psi_k|\,, \tag{11}$$

where $\{E_k\}$ are the eigenvalues of the Hamiltonian and $\{|\psi_k\rangle\}$ their corresponding eigenvectors.

The evolution of a single qubit by a time-independent Hamiltonian corresponds to a precession of the state on the Bloch sphere. The state will precess around an axis $\vec{n}$, which is an eigenvector of the Hamiltonian, with a angular speed ω. The Hamiltonian for this is

$$\mathcal{H} = \frac{\omega\hbar}{2}\vec{n}\cdot\vec{\sigma}, \tag{12}$$

where $\vec{\sigma}$ is the Pauli vector defined as $\vec{\sigma} = \sigma_x\vec{x} + \sigma_y\vec{y} + \sigma_z\vec{z}$,

3.2 Geometric phase

Consider the eigenvalue equation of the evolution from $t = 0$ to $t = \tau$

$$\mathcal{U}(\tau, 0)\,|\psi_k\rangle = \lambda_k\,|\psi_k\rangle\,. \tag{13}$$

This is a cyclic evolution where the state $|\psi_k\rangle$ evolves along a path on the Bloch sphere and ends up back where it started at time τ. Since $\mathcal{U}$ is unitary it follows that

$$\begin{aligned}\langle\psi_k|\,\mathcal{U}^\dagger\mathcal{U}\,|\psi_k\rangle &= \langle\psi_k|\,\lambda_k^*\lambda_k\,|\psi_k\rangle = |\lambda_k|^2\,\langle\psi_k|\psi_k\rangle\,, \\ \langle\psi_k|\,\mathcal{U}^\dagger\mathcal{U}\,|\psi_k\rangle &= \langle\psi_k|\,\mathcal{I}\,|\psi_k\rangle = \langle\psi_k|\psi_k\rangle\,,\end{aligned} \tag{14}$$

from which we see that

$$\begin{aligned} |\lambda_k|^2 &= 1 \\ \lambda_k &= e^{-i\varphi_k}. \end{aligned} \tag{15}$$

The eigenvalues of the evolution will therefore always be phase factors and φ_k will be the acquired phase after the cyclic evolution. This phase can be split up into two parts as [4]

$$\varphi_k = \delta_k + \gamma_k, \tag{16}$$

where δ_k is the dynamical phase and γ_k is the geometric phase. These phases are defined as

$$\delta_k = -\frac{1}{\hbar}\int_0^\tau \langle\psi_k|\,\mathcal{U}^\dagger(t,0)\mathcal{H}(t)\mathcal{U}(t,0)\,|\psi_k\rangle\,dt, \tag{17}$$

$$\gamma_k = \varphi_k - \delta_k = \arg\langle\psi_k|\,\mathcal{U}(\tau,0)\,|\psi_k\rangle + \int_0^\tau \langle\psi_k|\,\mathcal{U}^\dagger(t,0)\mathcal{H}(t)\mathcal{U}(t,0)\,|\psi_k\rangle\,dt. \tag{18}$$

By splitting up the phases in this fashion the geometric phase will be purely dependent on the geometry of the evolution and have no dependence on the rate of change along the path. For a qubit the geometric phase will be equal to the solid angle enclosed by the path on the Bloch sphere.

By using the relation in Eq. (11) the time evolution operator becomes

$$\mathcal{U}(\tau,0) = \sum_k e^{-i\varphi_k}\,|\psi_k\rangle\langle\psi_k| = \sum_k e^{-i(\delta_k+\gamma_k)}\,|\psi_k\rangle\langle\psi_k|\,. \tag{19}$$

For a two-dimensional case the time evolution operators will belong to the group $SU(2)$. From this it follows that the eigenvalues $\varphi_{0,1}$ will be $\varphi_{0,1} = \pm\varphi$. The path traced out by the qubit on the Bloch sphere will be mirrored. The enclosed solid angle from each of the eigenstates $|\psi_\pm\rangle$ will therefore be equal but with opposite normal vectors. It then follows that $\gamma_{0,1} = \pm\gamma$. From these two statements it also follows that $\delta_{0,1} = \pm\delta$. With this the matrix of the evolution in the basis of the eigenvectors is

$$\mathcal{U}(\tau,0) = \begin{pmatrix} e^{-i\varphi} & 0 \\ 0 & e^{i\varphi} \end{pmatrix} = \begin{pmatrix} e^{-i(\delta+\gamma)} & 0 \\ 0 & e^{i(\delta+\gamma)} \end{pmatrix} = e^{-i(\delta+\gamma)}\begin{pmatrix} 1 & 0 \\ 0 & e^{2i(\delta+\gamma)} \end{pmatrix}. \tag{20}$$

Just as before the factor $e^{-i(\delta+\gamma)}$ has no physical meaning.

3.3 Implementation of geometric quantum gates

For evolution where $2\delta = 0 \mod 2\pi$ we have $e^{2i\delta} = 1$. This results in $\varphi = \gamma$, meaning the total acquired phase is completely geometrical and equal to the enclosed solid angle on the Bloch sphere. One can notice that the final expression in Eq. (20) is a T-gate if $2\gamma = \pi/4$ and the eigenstates of $\mathcal{U}$ are used as computational basis. It is not only phase shift gates which can be implemented by geometric gates, but any gate is possible by letting the eigenvectors match the eigenvectors of the desired gate and 2γ be equal to its rotation.

The reason why creating quantum gates using only geometric phases is interesting is because they are naturally resilient to certain types of noise [5]. These gates are implemented by using pulses of effective fields $\vec{B}$ that drive the qubit.

$$\mathcal{H} = \frac{\hbar}{2}\vec{B} \cdot \vec{\sigma}. \tag{21}$$

The magnitude of $\vec{B}$ determines the rotational speed ω in Eq. (12), and the direction of $\vec{B}$ determines the axis of rotation $\vec{n}$. In a realistic scenario there will be some fluctuations in the field strength of the components of $\vec{B}$ resulting in noise of both ω and $\vec{n}$. Since the geometric phase is independent of the rate of change of the evolution, noise in ω will not directly contribute to noise in the gate. The noise in $\vec{n}$ will still affect the gate, as the path of the evolution will be altered. However, since the geometric phase is related to the enclosed solid angle of the path on the Bloch sphere, fluctuations around the path could cancel each other, resulting in the same enclosed solid angle. Geometric gates are therefore also somewhat resilient to noise in the $\vec{n}$.

One common way of implementing geometric gates are by letting the states evolve as geodesics, or portions of great circles, on the Bloch sphere [13]. When a state evolves along geodesics it gains no dynamical phase along the path and is because of this guaranteed to be geometric. A gate implemented by using two pulses can be made into a phase gate by having the two pulses both rotate the qubit an angle π, first around the y-axis and then around another axis of rotation lying in the xy-plane. The path these two pulses create form an orange slice of the Bloch sphere and the choice of the second axis of rotation dictates the size of the enclosed area. In Fig. 2 an example of such a gate can be seen, which in this case is a Z-gate.

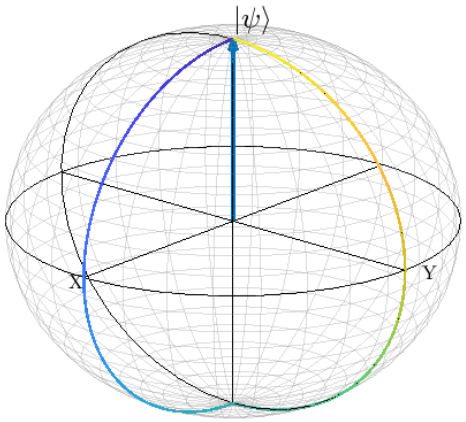

Figure 2: A geometric Z-gate implemented with two pulses. The path the qubit takes on the Bloch sphere gradually shifts from blue at the start to yellow at the end.

3.4 Non-cyclic geometric gates

While the resilience against errors associated with geometric gates are very desirable for quantum gates the operational time is also important. The information encoded in the qubit will eventually be lost to decoherence, undesired interactions with the environment [14]. Therefore, the operational time of the quantum computation must be shorter than the decoherence time. To reduce the operational time of geometric gates, non-cyclic schemes have been proposed [6–8]. The schemes make use of methods to remove the dynamical phase from the computational basis, while the basis evolve along open paths. However, since the paths are open the computational basis is no longer the eigenbasis of the

time evolution operator. The dynamical phase for the eigenvectors are in general non-trivial for these schemes and it is therefore questionable if they should be considered genuinely geometric.

For a non-cyclic gate to genuinely be considered geometric the eigenvectors of the time evolution operator should still fulfill the condition of evolving purely geometric, but it is also required for the computational basis to only acquire trivial dynamical phase to retain the error resilience. To ensure this one could construct gates where the computational states evolve along geodesic segments, ensuring they gain no dynamical phase during the evolution, and find for which of these paths the eigenvectors of the time evolution operators only gain trivial dynamical phase. Such gates are coined genuinely non-cyclic geometric gates.

4 Results

To implement non-cyclic geometric quantum gates, evolution generated by two pulses are used. The pulses move the computational basis along segments of geodesic paths. After constructing these gates, the dynamical phase of the eigenstates of the gate is studied, to find which gates are geometric, i.e., fulfilling the condition $2\delta = 2\pi n$.

For a path to be a geodesic on a sphere the axis of rotation must be orthogonal to the vector being rotated. Beginning in the $|0\rangle$ or $|1\rangle$ state all rotational axes lying in the xy-plane would create geodesic paths. The difference between choosing one axis over another would result in a phase shift. It is therefore sufficient to study one axis and then rotate the gate if needed. Therefore, the first pulse is chosen to always be a rotation around the y-axis, i.e., $\vec{n}_1 = \vec{y}$. According to Eq. (12), the Hamiltonian of this rotation takes the form

$$\mathcal{H}_1 = \frac{\omega\hbar}{2}\sigma_y, \tag{22}$$

resulting in the time evolution operator

$$\mathcal{U}_1(t,0) = \exp\left[-i\frac{\omega t}{2}\begin{pmatrix} 0 & -i \\ i & 0 \end{pmatrix}\right]. \tag{23}$$

To express this exponential in matrix form the eigenvalue and eigenvectors of the Hamiltonian are needed. These are

$$\lambda_\pm = \pm\frac{\hbar\omega}{2}, \tag{24}$$

$$|\kappa_{y\pm}\rangle = \frac{1}{\sqrt{2}}\begin{bmatrix} 1 \\ \pm i \end{bmatrix}. \tag{25}$$

The corresponding time evolution reads

$$\mathcal{U}_1(t,0) = |\kappa_{y+}\rangle\, e^{\frac{-i\omega t}{2}}\, \langle\kappa_{y+}| + |\kappa_{y-}\rangle\, e^{\frac{i\omega t}{2}}\, \langle\kappa_{y-}| = \begin{pmatrix} \cos\left(\frac{\omega t}{2}\right) & -\sin\left(\frac{\omega t}{2}\right) \\ \sin\left(\frac{\omega t}{2}\right) & \cos\left(\frac{\omega t}{2}\right) \end{pmatrix}. \tag{26}$$

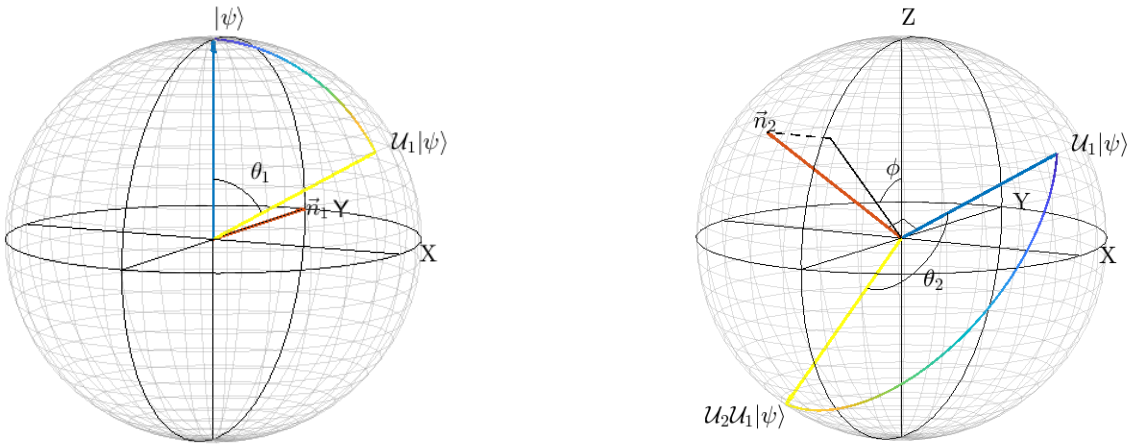

(a) (b)

Figure 3: a) The precession of the qubit during the first pulse. θ_1 is the precession angle and $\vec{n}_1$ is the axis of rotation. b) The precession of the qubit during the second pulse. θ_2 is the precession angle, ϕ determines the axis of rotation $\vec{n}_2$. $\vec{n}_2$ is also orthogonal to the final state of the first pulse, $\mathcal{U}_1|\psi\rangle$. The paths in both figures gradually shifts from blue at the start to yellow at the end.

At the final time t_1 the pulse has rotated the qubit an angle $\theta_1 = \omega t_1$. This precession can be seen in Fig. 3a. For the second pulse to move the qubit along a geodesic path the axis of rotation must be orthogonal to the final state of the first pulse. Starting at $|0\rangle$ the final state of the first pulse will have the coordinates $\sin\theta_1\vec{x} + \cos\theta_1\vec{z}$. The axis of rotations $\vec{n}$ of the second pulse is therefore

$$\vec{n}_2 = \sin(\theta_1 - \pi/2)\cos\phi\vec{x} + \sin\phi\vec{y} + \cos(\theta_1 - \pi/2)\cos\phi\vec{z}. \tag{27}$$

This lies in the plane spanned by a vector in the xz-plane, orthogonal to the final state of the qubit, and the y-axis. ϕ is the angle around the final state of the first pulse, determining which axis of rotation in this plane. With the axis of rotation defined the Hamiltonian becomes

$$\mathcal{H}_2 = \frac{\omega\hbar}{2}\left(-\cos\theta_1\cos\phi\,\sigma_x + \sin\phi\,\sigma_y + \sin\theta_1\cos\phi\,\sigma_z\right). \tag{28}$$

Once again the eigenvalues and eigenvectors of Hamiltonian must be found to write the time evolution operator on matrix form. They are

$$\lambda_\pm = \pm\frac{\hbar\omega}{2}, \tag{29}$$

$$|\kappa_\pm\rangle = \sqrt{\frac{\cos^2\theta_1\cos^2\phi + \sin^2\phi}{2 \mp 2\sin\theta_1\cos\phi}}\left[|0\rangle + \frac{\pm 1 - \sin\theta_1\cos\phi}{-\cos\theta_1\cos\phi - i\sin\phi}|1\rangle\right]. \tag{30}$$

The time evolution operator is

$$\mathcal{U}_2(t,0) = |\kappa_+\rangle\, e^{\frac{-i\omega t}{2}}\, \langle\kappa_+| + |\kappa_-\rangle\, e^{\frac{i\omega t}{2}}\, \langle\kappa_-| \tag{31}$$

$$= \begin{pmatrix} \cos\left(\frac{\omega t}{2}\right) - i\cos(\phi)\sin\left(\frac{\omega t}{2}\right) & -\sin(\phi)\sin\left(\frac{\omega t}{2}\right) \\ \sin(\phi)\sin\left(\frac{\omega t}{2}\right) & \cos\left(\frac{\omega t}{2}\right) + i\cos(\phi)\sin\left(\frac{\omega t}{2}\right) \end{pmatrix}. \tag{32}$$

Finally, the total time evolution operator $\mathcal{U}_{tot}$ is

$$\mathcal{U}_{tot}(t,0) = \begin{cases} \mathcal{U}_1(t,0), & 0 \le t \le t_1, \\ \mathcal{U}_2(t,t_1)\mathcal{U}_1(t_1,0), & t_1 \le t \le \tau, \end{cases} \tag{33}$$

where τ is the final time of the second pulse, at which point the qubit has rotated an additional angle $\theta_2 = \omega(\tau - t_1)$.

With the total time evolution operator we may now calculate the eigenvalues and eigenvectors of the evolution from time $t = 0$ to $t = \tau$. It is these which specify the gate. The eigenvalues are found by solving

$$\det(\mathcal{U}_2(\tau,t_1)\mathcal{U}_1(t_1,0) - \lambda\mathcal{I}) \tag{34}$$

$$= \begin{vmatrix} \cos\left(\frac{\theta_1}{2}\right)\left[\cos\left(\frac{\theta_2}{2}\right) - i\cos\phi\sin\left(\frac{\theta_2}{2}\right)\right] & \sin\left(\frac{\theta_1}{2}\right)\left[-\cos\left(\frac{\theta_2}{2}\right) + i\cos\phi\sin\left(\frac{\theta_2}{2}\right)\right] \\ -\sin\left(\frac{\theta_1}{2}\right)\sin\left(\frac{\theta_2}{2}\right)\sin\phi - \lambda & -\cos\left(\frac{\theta_1}{2}\right)\sin\left(\frac{\theta_2}{2}\right)\sin\phi \\ \sin\left(\frac{\theta_1}{2}\right)\left[\cos\left(\frac{\theta_2}{2}\right) + i\cos\phi\sin\left(\frac{\theta_2}{2}\right)\right] & \cos\left(\frac{\theta_1}{2}\right)\left[\cos\left(\frac{\theta_2}{2}\right) + i\cos\phi\sin\left(\frac{\theta_2}{2}\right)\right] \\ +\cos\left(\frac{\theta_1}{2}\right)\sin\left(\frac{\theta_2}{2}\right)\sin\phi & -\sin\left(\frac{\theta_1}{2}\right)\sin\left(\frac{\theta_2}{2}\right)\sin\phi - \lambda \end{vmatrix} = 0. \tag{35}$$

This gives

$$\lambda_\pm = \cos\left(\frac{\theta_1}{2}\right)\cos\left(\frac{\theta_2}{2}\right) - \sin\left(\frac{\theta_1}{2}\right)\sin\left(\frac{\theta_2}{2}\right)\sin\phi \tag{36}$$

$$\pm i\sqrt{1 - \left[\cos\left(\frac{\theta_1}{2}\right)\cos\left(\frac{\theta_2}{2}\right) - \sin\left(\frac{\theta_1}{2}\right)\sin\left(\frac{\theta_2}{2}\right)\sin\phi\right]^2} \equiv e^{\pm i\varphi}. \tag{37}$$

The corresponding eigenvectors are

$$\left|\tilde{\psi}_\pm\right\rangle = |0\rangle + \frac{\cos\left(\frac{\theta_1}{2}\right)\left[-\cos\left(\frac{\theta_2}{2}\right) + i\cos\phi\sin\left(\frac{\theta_2}{2}\right)\right] + \sin\left(\frac{\theta_1}{2}\right)\sin\left(\frac{\theta_2}{2}\right)\sin(\phi) + e^{\pm i\varphi}}{\sin\left(\frac{\theta_1}{2}\right)\left[-\cos\left(\frac{\theta_2}{2}\right) + i\cos\phi\sin\left(\frac{\theta_2}{2}\right)\right] - \cos\left(\frac{\theta_1}{2}\right)\sin\left(\frac{\theta_2}{2}\right)\sin\phi}\,|1\rangle\,. \tag{38}$$

The normalization is

$$\frac{1}{\left\langle \tilde{\psi}_{\pm} \middle| \tilde{\psi}_{\pm} \right\rangle} \tag{39}$$
$$= \frac{2 - \cos\theta_1 \left[1 + \cos\theta_2 + 2\cos(2\phi)\sin\left(\frac{\theta_2}{2}\right)^2\right] + 2\sin\theta_1 \sin\theta_2 \sin(\phi)}{8\left(1 + \cos\left(\frac{\theta_1}{2}\right)\left[-\cos\left(\frac{\theta_2}{2}\right)\cos\varphi \pm \sin\left(\frac{\theta_2}{2}\right)\cos\phi\sin\varphi\right] + \sin\left(\frac{\theta_1}{2}\right)\sin\left(\frac{\theta_2}{2}\right)\sin\phi\cos\varphi\right)},$$

which gives the normalized eigenvectors

$$|\psi_{\pm}\rangle = \frac{1}{\sqrt{\left\langle \tilde{\psi}_{\pm} \middle| \tilde{\psi}_{\pm} \right\rangle}} \left|\tilde{\psi_{\pm}}\right\rangle. \tag{40}$$

Next we find the dynamical phases of the evolution. The dynamical phase is calculated by using Eq. (17), which yields

$$\delta_{\pm} = -\frac{1}{\hbar}\int_0^{t_1} \langle\psi_{\pm}|\,\mathcal{U}_1^{\dagger}(t,0)\mathcal{H}_1(t)\mathcal{U}_1(t,0)\,|\psi_{\pm}\rangle\,dt \tag{41}$$
$$-\frac{1}{\hbar}\int_{t_1}^{\tau} \langle\psi_{\pm}|\,\mathcal{U}_1^{\dagger}(t_1,0)\mathcal{U}_2^{\dagger}(t,t_1)\mathcal{H}_2(t)\mathcal{U}_2(t,t_1)\mathcal{U}_1(t,0)\,|\psi_{\pm}\rangle\,dt. \tag{42}$$

The Hamiltonians $\mathcal{H}_1$ and $\mathcal{H}_2$ commutate with $\mathcal{U}_1$ and $\mathcal{U}_2$, respectively. This can be used in the following manner:

$$\mathcal{U}_1^{\dagger}(t,0)\mathcal{H}_1(t)\mathcal{U}_1(t,0) = \mathcal{U}_1^{\dagger}(t,0)\mathcal{U}_1(t,0)\mathcal{H}_1(t) = \mathcal{I}\mathcal{H}_1(t) = \frac{\omega\hbar}{2}\sigma_y, \tag{43}$$

and

$$\mathcal{U}_1^{\dagger}(t_1,0)\mathcal{U}_2^{\dagger}(t,t_1)\mathcal{H}_2(t)\mathcal{U}_2(t,t_1)\mathcal{U}_1(t_1,0) = \mathcal{U}_1^{\dagger}(t_1,0)\mathcal{H}_2(t)\mathcal{U}_1(t_1,0). \tag{44}$$

Explicitly calculating Eq. (44) it is found to be

$$\mathcal{U}_1^{\dagger}(t_1,0)\mathcal{H}_2(t)\mathcal{U}_1(t,0) = \frac{\omega\hbar}{2}\left(-\cos\phi\sigma_x + \sin\phi\sigma_y\right). \tag{45}$$

This shows that none of the integrands are time-dependent and the integrals become

$$\delta_{\pm} = -\frac{\theta_1}{2}\langle\psi_{\pm}|\,\sigma_y\,|\psi_{\pm}\rangle - \frac{\theta_2}{2}\langle\psi_{\pm}|\left(-\cos\phi\sigma_x + \sin\phi\sigma_y\right)|\psi_{\pm}\rangle. \tag{46}$$

To find geometric gates we need to solve for which choices of θ_1, θ_2, and ϕ the dynamical phases become trivial, i.e., fulfilling the condition $2\delta = 2\pi n$. To find the parameters when this is fulfilled a root-finding algorithm is used on the equation

$$-\theta_1\langle\psi_{\pm}|\,\sigma_y\,|\psi_{\pm}\rangle - \theta_2\langle\psi_{\pm}|\left(-\cos\phi\sigma_x + \sin\phi\sigma_y\right)|\psi_{\pm}\rangle - 2\pi n = 0. \tag{47}$$

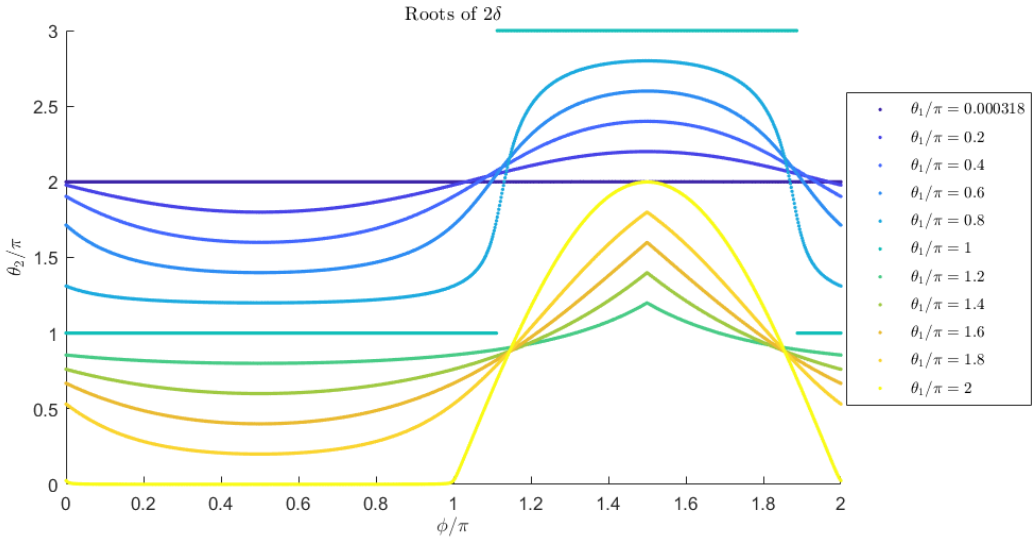

Figure 4: The roots of $2\delta = 0$. θ_1 (θ_2) is the first (second) precession angle, and ϕ is the angle determining the axis of rotation for the second precession.

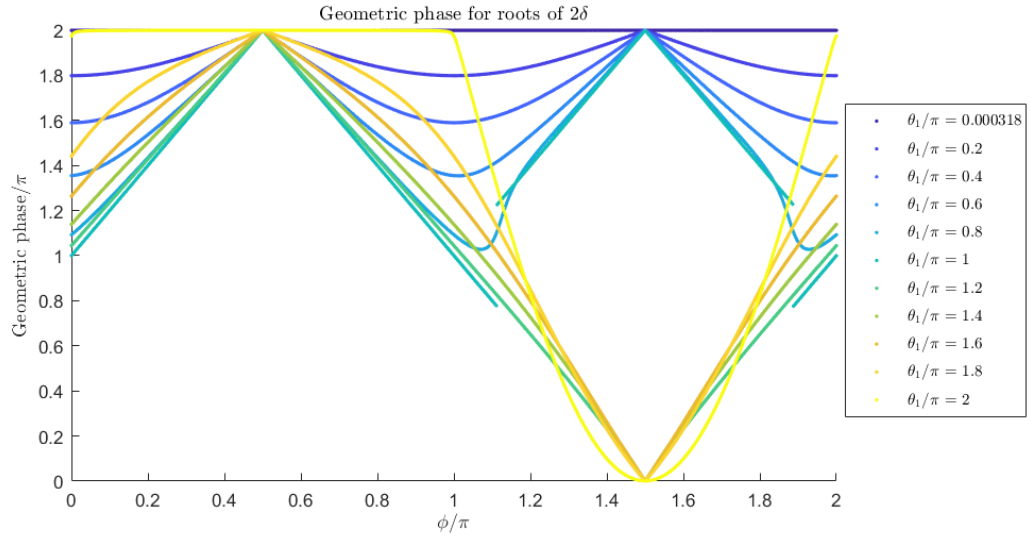

Figure 5: The geometric phase corresponding to the roots of $2\delta = 0$. θ_1 is the first precession angle, θ_2 is the second precession angle, and ϕ is the angle determining the axis of rotation for the second precession.

The time necessary to perform the evolution is proportional to the total angle of the two precessions. Therefore, the roots with the smallest total precession angles are the most relevant. For this evolution the smallest total precession angles are found when $n = 0$, i.e., $2\delta = 0$. The roots of the dynamical phase for some parameters are plotted in Fig. 4. From the figure one can see that the total precession angle always equals 2π or more. In Fig. 5 the corresponding geometric phase for the roots are shown. It is possible to find all geometric phases ranging from 0 to 2π. It should be noted that geometric phases smaller than π are only found when ϕ and θ_1 are larger than π and the total precession angle of these path are larger than 2π.

Since it is not only the geometric phase, but also the eigenvectors, that define what gate the evolution corresponds to, these vectors are also important. To be able to implement any gate using only two pulses any combination of geometric phase and eigenvector must be possible. To study this the eigenvectors of all gates with $2\gamma = \pi$ are plotted as shown in Fig. 6. The z-values of these vectors cover the entire z-axis. It is also important to remember that only gates with the first rotation taken around the y-axis has been considered so far. By changing the first axis of rotation to another axis in the xy-plane, but keeping the relation between the first and second axis, the system would be phase shifted, meaning the eigenvectors would be rotated about the z-axis. Any gate with π-rotations can then be implemented. This can similarly be shown for gates with rotations other than $2\gamma = \pi$.

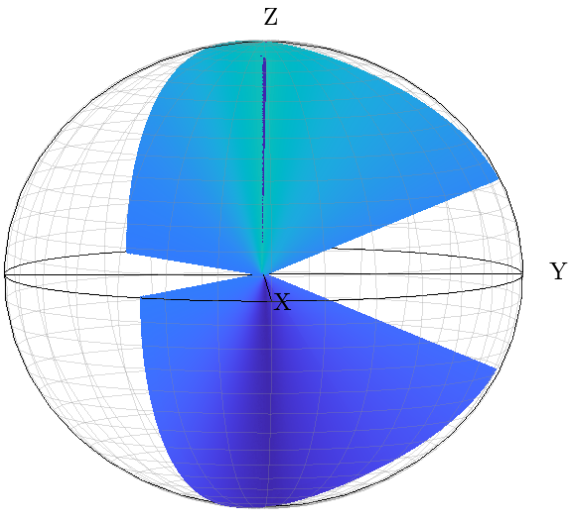

Figure 6: The eigenvectors of all gates with $2\gamma = \pi$ with the first rotation taken around the y-axis.

To give an example, we show how a Hadamard gate can be implemented. This gate is a π-rotation around the axis $\frac{\vec{x}+\vec{z}}{\sqrt{2}}$, meaning an evolution with $2\gamma = \pi$ and an eigenvector in that direction is needed. In Fig. 6, no vector in that direction can be found, but an eigenvector with the same polar angle as $\frac{\vec{x}+\vec{z}}{\sqrt{2}}$ can. The path created by the gate, with this

eigenvector, acting upon its eigenvector and the $|0\rangle$-state can be seen in Fig. 7. In Fig. 7b, we see that the $|0\rangle$-state is mapped onto a state on the xy-plane, but not the $\frac{|0\rangle+|1\rangle}{\sqrt{2}}$-state, which is where the Hadamard gate would map it unto. To change this gate into a Hadamard gate we want to rotate the axes of rotation of this gate around the z-axis with the difference in azimuthal angle between the eigenvector and $\frac{\vec{x}+\vec{z}}{\sqrt{2}}$. The eigenvector of the rotated gate will be phase shifted by the same angle, shifting it into $\frac{\vec{x}+\vec{z}}{\sqrt{2}}$, resulting in turning it into a Hadamard gate. The paths of the new eigenvector and the $|0\rangle$-state acted upon by the Hadamard gate is shown in Fig. 8.

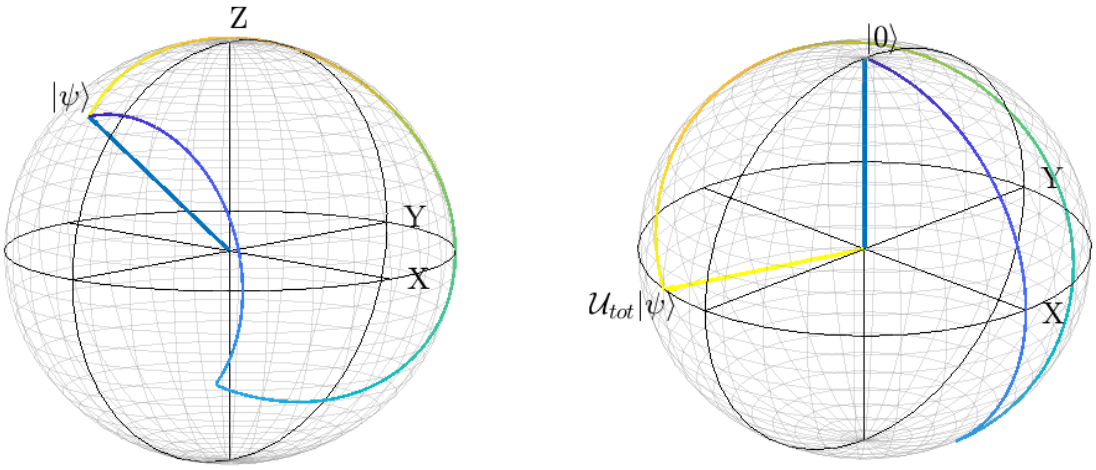

(a) (b)

Figure 7: a) The path of one of the eigenstates of a gate with $2\gamma = \pi$. The eigenstates has the same polar angles as the eigenstates of the Hadamard gate. b) The path of the $|0\rangle$-state with the same gate acted upon it.

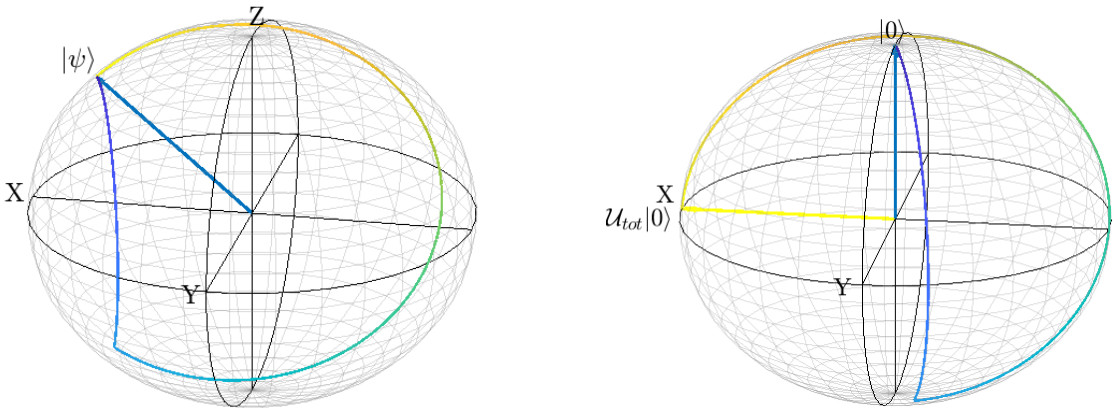

(a) (b)

Figure 8: The path of one of the eigenstates (a) and the $|0\rangle$-state (b) when acted upon by a geometric Hadamard gate. The computational state evolves along geodesic segments.

5 Discussion and conclusions

We have shown here that it is possible to create two pulse non-cyclic geometric gates, where the computational states evolve along open paths consisting of two geodesic segments, and the paths are chosen such that the eigenvectors of the time evolution operators only gain trivial dynamical phase. With this scheme, both the computational basis and the eigenvectors pick up no dynamical phase and the gates can be called genuinely non-cyclic geometric gates. This further improves upon the understanding of what constitutes geometric gates and how they can be found for the non-cyclic case.

It was not possible to find gates with shorter operation times than for cyclic gates, as all non-cyclic gates found, had a total precession angle equal to or larger than 2π. For this reason there were no gain in this respect, which was the reason the previous schemes were proposed. These finding are, however, still important. It is only phase gates that are cyclic in regards to the computational basis, but for universal computations gates other than phase gates are also required. For example, the Hadamard gate maps the $|0\rangle$-state to the $\frac{|0\rangle+|1\rangle}{\sqrt{2}}$. With the scheme found in this report, geometric implementations can be found for these non-cyclic gates as well.

This study has been limited to gates using only two pulses. However, this method of finding geometric gates could be extended to three or more pulses. The main gain possible with introducing more pulses is potential reduction in the total precession angle. The total precession angle is related to the time necessary for the evolution. Reducing the operation time of the gate reduces the time the qubits' are exposed to the environment and thereby reduce their decoherence. The drawback in introducing more pulses can be added noise from the additional pulses. Because of this the reduction in decoherence must be balanced against a possible increase in noise. It is also possible to expand the scheme to evolution

where the computational basis evolves along non-geodesic paths. In this case it would be necessary to condition the paths such that both the eigenstates and the computational basis to gain trivial dynamical phases but the removal of the condition of geodesic evolution would increase the degrees of freedom in choosing the evolution. The reason to introduce non-geodesic paths would also be to find paths with smaller total precession angles.

To showcase the scheme developed here on a experimental setup, qubits based on, for example, trapped ions or nitrogen cavity centers would be natural choices. This is because they are controlled with pulses of lasers. These pulses are good for applying the piece-wise constant Hamiltonians used to implement the gates showed here.

In summary, this report have shown how genuinely geometric non-cyclic gates can be implemented, demonstrating how geometric gates can be used for general quantum computations. Further improvements could be made by altering the scheme to try and reduce the operational time of the gates. Lastly, a experimental demonstration would be needed to actuate the scheme.

References

[1] P. Shor, Polynomial-Time algorithms for prime factorization and discrete logarithms on a quantum computer, SIAM Review **26**, 303 (1997).

[2] M. Nielsen and I. Chuang, Quantum computation and quantum information: 10th anniversary edition, (Cambridge University Press, Cambridge).

[3] A. Ekert, M. Ericsson, P. Hayden, H. Inamori, J. A. Jones, D. K. L. Oi, and V. Vedral, Geometric Quantum Computation, J. Mod. Opt. **47**, 2501 (2000).

[4] Y. Aharonov and J. Anandan, Phase change during a cyclic quantum evolution, Phys. Rev. Lett. **58**, 1593 (1987).

[5] S. Berger, M. Pechal, A. A. Abdumalikov, Jr., C. Eichler, L. Steffen, A. Fedorov, A. Wallraff, and S. Filipp, Exploring the effect of noise on the berry phase, Phys. Rev. A **58**, 060303 (2013).

[6] A. Friedenauer and E. Sjöqvist, Noncyclic geometric quantum computation, Phys. Rev. A **67**, 024303 (2003).

[7] B. Liu, S. Su, and M. Yung, Nonadiabatic noncyclic geometric quantum computation in Rydberg atoms, Phys. Rev. Res. **2**, 043130 (2020).

[8] L. Qiu, H. Li, Z. Han, W. Zheng, X. Yang, Y. Dong, S. Song, D. Lana, X. Tana, and Y. Yu, Experimental realization of noncyclic geometric gates with shortcut to adiabaticity in a superconducting circuit, Appl. Phys. Lett. **118**, 254002 (2021).

[9] L.-M. Duan, J. I. Cirac, P. Zoller, Geometric manipulation of trapped ions for quantum computation, Science **292**, 5522 (2001).

[10] F. Kleißler, A. Lazariev, and S. Arroyo-Camejo, Universal, high-

delity quantum gates based on superadiabatic, geometric phases on a solid-state spin-qubit at room temperature, npj Quantum Info. **4**, 49 (2018).

[11] Y. Xu, Z. Hua, T. Chen, X. Pan, X. Li, J. Han, W. Cai, Y. Ma, H.Wang, Y. P. Song, Z.-Y. Xue, and L. Sun, Experimental Implementation of Universal Nonadiabatic Geometric Quantum Gates in a Superconducting Circuit, Phys. Rev. Lett. **124**, 230503 (2020).

[12] J.J. Sakurai and J. Napolitano, Modern quantum mechanics: second edition, (Addison-Wesley, Reading).

[13] M. Tian, Z. W. Barber, J. A. Fischer, and W. R. Babbitt, Geometric manipulation of the quantum states of two-level atoms, Phys. Rev. A **69**, 050301(R) (2004).

[14] D. DiVincenzo, Quantum computation, Science **270**, 5234 (1995)